Articles

The Formylglycinamide Ribonucleotide Amidotransferase Complex from *Bacillus subtilis*: Metabolite-Mediated Complex Formation†

Aaron A. Hoskins,‡ Ruchi Anand,§ Steven E. Ealick,§ and JoAnne Stubbe*,‡,||

Department of Chemistry, Massachusetts Institute of Technology, Cambridge, Massachusetts 02139, Department of Chemistry and Chemical Biology, Cornell University, Ithaca, NewYork 14853, and Department of Biology, Massachusetts Institute of Technology, Cambridge, Massachusetts 02139

Received April 29, 2004; Revised Manuscript Received June 12, 2004

ABSTRACT: Formylglycinamide ribonucleotide amidotransferase (FGAR-AT) catalyzes the ATP- and glutamine-dependent formation of formylglycinamidine ribonucleotide, ADP, P_i, and glutamate in the fourth step of de novo purine biosynthesis. Like all amidotransferases (ATs), FGAR-AT is proposed to channel ammonia between a glutaminase and AT domain. In Gram-negative bacteria and eukaryotes, FGAR-AT is a single ∼140 kDa protein. In archae and Gram-positive bacteria, the FGAR-AT is formed from three proteins: PurS (10 kDa), PurQ (25 kDa, a glutaminase), and smPurL (80 kDa, an AT). This is the only known AT to require a third structural component (PurS) for activity. Here we report the first purification and biochemical characterization of a three-component AT from *Bacillus subtilis*. Efforts to isolate an intact FGAR-AT focused initially on coexpression of PurS, smPurL, and PurQ. However, all attempts to purify the complex resulted in separation of the constituent proteins. PurS, smPurL, and PurQ were therefore separately expressed and purified to homogeneity. PurQ had a glutaminase activity of 0.002 s^{-1}, and smPurL had an ammonia-dependent AT activity of 0.044 s^{-1}. Reconstitution of PurS, smPurL, and PurQ at a ratio of 2:1:1 gave an activity of 2.49 s^{-1}, similar to that previously reported for the *Escherichia coli* 140 kDa FGAR-AT (5.00 s^{-1}). PurS was essential for the glutamine-dependent FGAR-AT activity. Surprisingly, activity was found to be absolutely dependent on the presence of Mg^{2+} and ADP, and a stable FGAR-AT complex of 2PurS/1smPurL/1PurQ was detected only in the presence of Mg^{2+}, ADP, and glutamine. The implications of these observations are discussed with respect to ammonia channeling.

The purine biosynthetic pathway requires 11 enzymatic transformations in prokaryotes, each of which has been studied in detail. With the exception of the fourth enzyme in this pathway, formylglycinamide ribonucleotide amidotransferase (FGAR-AT or PurL),[1] all of the enzymes have previously been structurally characterized as well (*1*). FGAR-AT catalyzes the transformation shown in Scheme 1 in which glutamine supplies the ammonia to an ATP-activated, formylglycinamide ribonucleotide (FGAR) to generate ADP, inorganic phosphate (P_i), glutamate, and formylglycinamidine ribonucleotide (FGAM). This reaction can be divided into two half-reactions. In one half-reaction, glutamine is hydrolyzed to glutamate through a covalent thioester intermediate (eq 1). In the second half-reaction, ATP is proposed to activate the amide oxygen of FGAR for nucleophilic attack by the ammonia generated in the first half-reaction (eq 2) (*1*).

$$\mathrm{Gln} + \mathrm{H_2O} \rightarrow \mathrm{Glu} + \mathrm{NH_3} \quad (1)$$

$$\mathrm{FGAR} + \mathrm{ATP} + \mathrm{NH_3} \rightarrow \mathrm{FGAM} + \mathrm{ADP} + \mathrm{P_i} \quad (2)$$

Recently, interest in FGAR-ATs has resurfaced for several reasons. First, the most extensively studied PurLs, those isolated from *Eschericia coli* and chicken liver, are monomers of MW 140 kDa (lgPurLs). The large size, more than adequate to convert an amide to an amidine (Scheme 1), has led to the hypothesis that this protein might serve as a scaffold to organize the 11 proteins involved in a purine biosynthetic metabolon (*1*). No evidence for "tight" interactions have been reported for the proteins in this pathway (*2*, *3*). However, the instability of many of the nucleotide intermediates has led to a model in which transient protein−protein interactions between successive enzymes in this pathway may be important to avoid nucleotide decomposition (*1*).

Second, our recent studies on the structure and function of the fifth enzyme in the purine pathway, aminoimidazole

† Supported by NIH Grant GM32191 to J.S. A.A.H was supported by a NSF predoctoral fellowship. A.A.H and J.S. were supported by NIH Grant GM32191.

* Corresponding author. Tel: +1-617-253-1814. Fax: +1-617-258-7247; E-mail: stubbe@mit.edu.

‡ Department of Chemistry, Massachusetts Institute of Technology.

§ Department of Chemistry and Chemical Biology, Cornell University.

|| Department of Biology, Massachusetts Institute of Technology.

10.1021/bi049127h CCC: $27.50
Published on Web 07/23/2004

Scheme 1

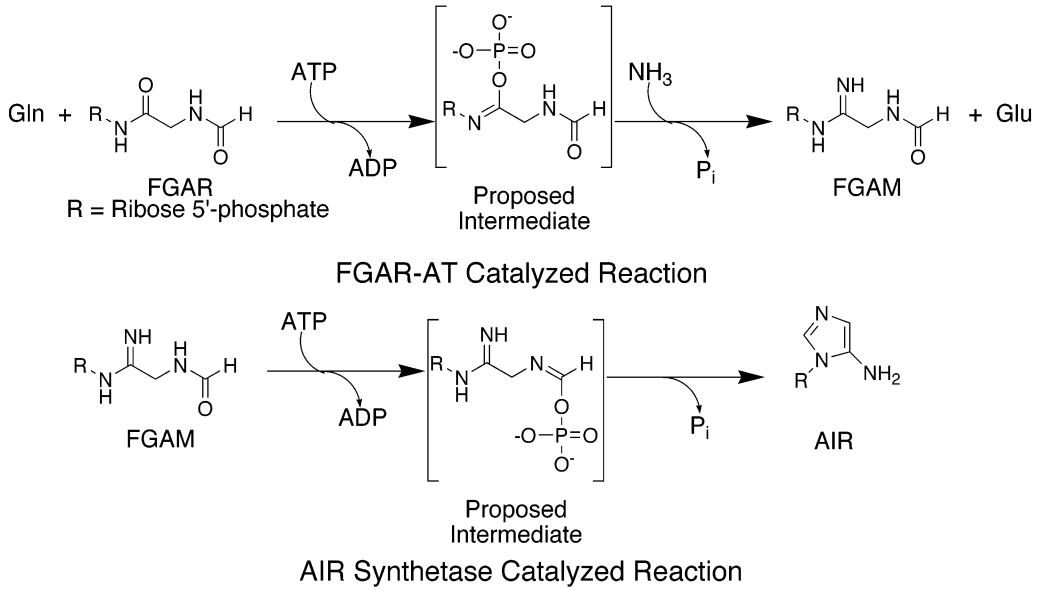

ribonucleotide (AIR) synthetase (PurM, Scheme 1), in conjunction with genomic sequence information, suggested that PurL might be a member of a new superfamily of ATP-requiring enzymes with a unique structural fold (*4*, *5*). This superfamily of enzymes was proposed to use ATP to phosphorylate an amide oxygen of its substrate to generate an iminophosphate intermediate that is activated for nucleophilic attack (Scheme 1). Further information on the structure and function of the FGAR-AT would shine light on this proposal.

As noted above, most of the mechanistic studies on the FGAR-AT have focused on the lgPurLs. In the 1980s, Zalkin and co-workers, studying the contiguous purine biosynthetic operon in *Bacillus subtilis*, sequenced a gene cluster that was composed of *purC*-orf-*purQ*-*purL*-*purF* (*6*). The *purL* gene coded for a protein of only 80 kDa and hence was designated small PurL (smPurL). Furthermore, *purQ* was found to be homologous to triad glutaminase domains including the glutaminase domain of lgPurLs. Recently genetic and biochemical studies by Saxild and Nygaard demonstrated that the orf within this gene cluster is essential for production of FGAM (*7*). This orf has now been designated *purS*. Thus it appears that three proteins (smPurL (80kDa), PurQ (25 kDa), and PurS (10 kDa)) form the *B. subtilis* FGAR-AT. Sequence gazing has further identified PurS homologues in a wide range of Gram-positive bacteria, cyanobacteria, and methanogens. In each case, *purS* is accompanied by a *purL* and a *purQ*. Our difficulties in obtaining a structure and elucidating the mechanism of the lgPurLs suggested that the FGAR-AT involving three proteins might be an alternative source of insight into the amidation process. As an initial step toward this goal, this paper describes the first expression and characterization of the FGAR-AT complex from *B. subtilis*. This FGAR-AT complex, as with all ATs examined to date, is proposed to supply ammonia from glutamine to FGAR by a channeling mechanism (*8*). This enzyme may therefore provide a paradigm for thinking about the dynamics of protein−protein interactions in channeling of an unstable intermediate in an enzymatic complex as well as between successive enzymes in primary metabolic pathways.

EXPERIMENTAL PROCEDURES

Materials. All reagents were purchased from Sigma or Mallinckrodt and used without further purification unless otherwise indicated. 6-Diazo-5-oxo-L-norleucine (DON) was purchased from BACHEM. Isopropyl β-D-thiogalactoside (IPTG) was purchased from Roche. β-FGAR was prepared from chemically synthesized α/β-GAR using the non-folate-dependent glycinamide ribotide transformylase, PurT (*9*). The PurT plasmid was a gift from H. Holden, University of Wisconsin-Madison (*10*). L-Glutamine was purchased from Fluka and found to contain the lowest percentage of contaminating L-glutamate among commercial sources. DNA primers were obtained from either the MIT Biopolymers Facility or Invitrogen and were desalted before use. All cloned genes were sequenced at the MIT Biopolymers Facility. ESI-MS and N-terminal protein sequencing were also performed at the MIT Biopolymers Facility. PurM containing a N-terminal histidine tag (MGSSHHHHHHSSGLVPRGSH) was purified as previously described (his-PurM, specific activity of 1−2 U/mg) (*4*). The *E. coli* and *Salmonella typhimurium* lgPurL enzymes (2 and 3 U/mg,

[1] Abbreviations: GAR, glycinamide ribonucleotide; FGAR, formylglycinamide ribonucleotide; FGAM, formylglycinamidine ribonucleotide; AIR, aminoimidazole ribonucleotide; AT, amidotransferase; FGAR-AT, formylglycinamide ribonucleotide amidotransferase; smPurL, small PurL subunit of the FGAR-AT complex; lgPurL, single subunit FGAR-ATs; PurM, AIR synthetase; HisHF, imidazole glycerol phosphate synthase; CPS, carbamoyl phosphate synthetase; PabAB, *p*-aminodeoxychorismate synthase; orf, open reading frame; BSA, bovine serum albumin; PK, rabbit muscle pyruvate kinase; LDH, rabbit muscle lactate dehydrogenase; GDH, bovine glutamate dehydrogenase; LB, Luria-Bertani media; EDTA, ethylenediamine tetraacetic acid; Tris, tris(hydroxymethyl)aminomethane; HEPES, *N*-2-hydroxyethylpiperazine-*N*′-2-ethanesulfonic acid; MES, 2-(*N*-morpholino)ethanesulfonic acid; MOPS, 3-(*N*-morpholino)propanesulfonic acid; TAPS, *N*-[tris-(hydroxymethyl)methyl]-3-aminopropanesulfonic acid; CHES, 2-(cyclohexylamino)ethanesulfonic acid; KP_i, potassium phosphate; ATP, adenosine 5′-triphosphate; ADP, adenosine 5′-diphosphate; PEP, phosphoenolpyruvate; NADH, reduced β-nicotinamide adenine dinucleotide; APAD, acetylpyridine adenine dinucleotide; DON, 6-diazo-5-oxo-L-norleucine; PCR, polymerase chain reaction; ESI-MS, electrospray ionization mass spectrometry; SEC, size exclusion chromatography; U, units of enzymatic activity (μmol/min); MW, molecular weight.

Table 1: Copurification of the FGAR-AT Complex

step	protein (mg)	total units (U)	SA (U/mg)	% yield
cell lysate[a]	399	167.6	0.42	100
streptomycin	328	127.9	0.39	76
DEAE Sepharose	84	22.7	0.27	14
Sephacryl S-200	9.6	0.12	0.013	0.1

[a] From 4 g of cells.

respectively) were purified as described (*11*, *12*). Pyruvate kinase (PK) and lactate dehydrogenase (LDH) were used from a premixed glycerol solution (660 U/mL PK, 1350 U/mL LDH Sigma P-0294). Bovine L-glutamate dehydrogenase (GDH) was obtained from Sigma (49 U/mg, Sigma G-2626). All spectrophotometric assays were performed on either a Cary 3 or a Cary 118-OLIS spectrophotometer. In both cases, the temperature was regulated using a Lauda water bath. Protein concentrations were determined using the method of Lowry with a BSA standard unless otherwise indicated (*13*). Calculated extinction coefficients were obtained using the ProtParam program from the EXPASY website (www.expasy.ch). To examine the extent of protein purification, standard SDS−PAGE gels were employed (10% for smPurL and 12.5% for PurQ). Tricine gels (16.5%) were used with PurS (*14*). A Bio-Rad BioLogic LP system was used for protein purifications at 4 °C using the procedures mentioned below.

Cloning of the B. subtilis FGAR-AT Components. PurS was cloned from isolated *B. subtilis* genomic DNA (*B. subtilis* strain no. 1A607, courtesy of A. Grossman, MIT). The gene was cloned using the AmpliTaq DNA polymerase (Perkin-Elmer) and the primers listed in Supplemental Table 1 (primers 1 and 2, Supporting Information). The gene was then ligated into the pET-11a vector (Novagen) at the *Nde*I and *Bam*HI sites. This construct yielded pET-PurS.

PurQ was also cloned from the isolated *B. subtilis* genomic DNA. The gene was first subcloned into pSTBlue-1 (Novagen) (primers 3 and 4, Supplemental Table 1, Supporting Information). Amplification with the VENT DNA polymerase (NEB) resulted in an A128T mutant of PurQ. Amplification with the AmpliTaq DNA polymerase (Perkin-Elmer) or the KOD HiFi DNA polymerase (Novagen) resulted in the cloning of the wild type (wt) gene. Both genes were then subcloned into pET-24a (Novagen) at the *Nde*I and *Eco*RI sites creating pET-PurQ-A128T (A128T mutant) and pET-PurQ-wt.

smPurL was cloned from the pDE51 *B. subtilis* sequencing vector (gift of H. Zalkin, Purdue University) (*6*). The gene was cloned using the *Pfu* Turbo DNA polymerase (Stratagene) and standard PCR techniques (primers 5 and 6, Supplemental Table 1, Supporting Information). The gene was ligated into the pET 24a vector at the *Nde*I and *Bam*HI sites to create pET-smPurL. The gene isolated by this procedure several times always contained a L513F mutation based on the published sequence (*6*).

To coexpress all the FGAR-AT components, PurQ A128T and smPurL were placed into pACYC-DUET-1 (Novagen). This vector contains two multiple cloning sites (MCS1 and MCS2) and is compatible with all pET vectors. The gene for smPurL was PCR-amplified from pET-smPurL (primers 6 and 7, Supplementary Table 1, Supporting Information) and placed into the *Nco*I and *Bam*HI sites of MCS1, creating pDUET-L. This method resulted in the insertion of an amino acid at the N-terminus: Met-Ser-Leu was replaced by Met-Gly-Ser-Leu. The gene for PurQ was amplified from pET-PurQ-A128T plasmid (primers 8 and 9, Supplementary Table 1, Supporting Information) and placed into MCS2 of pDUET-L at the *Nde*I and *Kpn*I sites to create pDUET-LQ.

Coexpression PurS, PurQ, and smPurL. For coexpression of all three subunits of the FGAR-AT, BL21-Gold DE3 cells (Stratagene) were transformed with pDUET-LQ, pET-PurS, and pET-smPurL using the heat-shock method and ∼20 ng of each plasmid (*15*). The cells were selected for growth on LB/agar plates containing 100 μg/mL chloramphenicol, 50 μg/mL ampicillin, and 35 μg/mL kanamycin.

A single colony was used to inoculate 50 mL of LB containing the above antibiotics. The cells were grown overnight at 37 °C with shaking at 200 rpm. Cells from this culture were then collected by centrifugation, washed with fresh LB, and then used to inoculate 2 L of LB containing the above mixture of antibiotics in a 6 L flask. This flask was then shaken at 200 rpm at 37 °C. Cells were grown to an OD_{600} of 0.7, at which point they were induced with 1 mM IPTG and grown for an additional 5 h. The cells were then harvested and frozen in liquid nitrogen.

Efforts to Purify FGAR-AT from Coexpressed Genes. Glutamine-dependent FGAR-AT activity was monitored at all stages of the purification with the modified Bratton−Marshall assay described below. Cells (4 g) were resuspended in 25 mL of SL buffer (50 mM Tris, 25 mM NaCl, 1 mM EDTA, 1 mM DTT, 5% glycerol, pH 7.8) along with 1 mL of Sigma Protease Inhibitor Cocktail (Sigma P-8465). Cells were then lysed by two passes through a French press at 14 000 psi. Cell debris was removed by centrifugation for 25 min at 17 000 rpm. Streptomycin sulfate (0.2 volumes, 6% w/v in SL buffer) was then added over 15 min, followed by stirring for an additional 15 min. Solids were removed by centrifugation.

The supernatant was next applied to a DEAE Sepharose FF (2.5 cm × 10 cm, Sigma) column equilibrated in SL buffer. The column was washed until $A_{280} < 0.1$. The protein was eluted with a linear gradient (350 × 350 mL) of 25−500 mM NaCl in SL buffer. A flow rate of 2 mL/min was used, and 8 mL fractions were collected. The proteins eluted in three separate peaks: PurS (∼100 mM NaCl), PurQ (∼150 mM NaCl), and smPurL (∼180 mM NaCl) (Figure 1). Glutamine-dependent FGAR-AT activity was observed in fractions at ∼170 mM NaCl. These fractions (41−53) were pooled and concentrated to 40 mg/mL using a YM-3 Centriprep (Millipore). This protein (0.5 mL) was then applied to a Sephacryl S-200 (1.5 cm × 100 cm, Sigma) column equilibrated in SL buffer. The column was eluted at 0.3 mL/min, and 5 mL fractions were collected and assayed for activity (Figure 2).

Purification of PurS. pET-PurS was transformed into BL21(DE3) *E. coli* cells (Novagen) and grown in LB at 37 °C in the presence of 100 μg/mL ampicillin. The cells were typically grown in 2 L with shaking at 200 rpm in a 6 L flask. At an OD_{600} of 0.7−0.9, the cells were induced with 1 mM IPTG and grown for an additional 4 h. The cells were then harvested and frozen in liquid nitrogen.

The cell pellet (6.5 g) was resuspended in 30 mL of S buffer (50 mM Tris, 25 mM NaCl, 1 mM EDTA, 5 mM

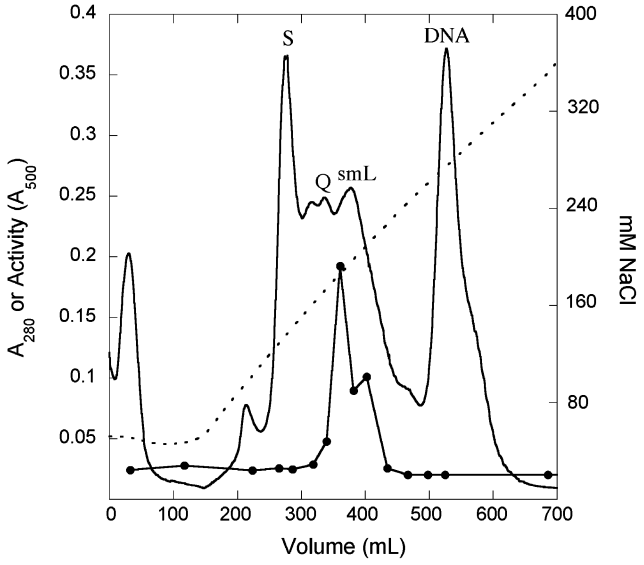

FIGURE 1: DEAE elution chromatogram of the coexpressed FGAR-AT complex. The solid line represents the A_{280} values, and the dashed line represents the NaCl concentration. Activity (●) was measured as A_{500} using the glutamine-dependent Bratton−Marshall assay. The elution of PurS (S), PurQ (Q), smPurL (smL), and cellular DNA are noted.

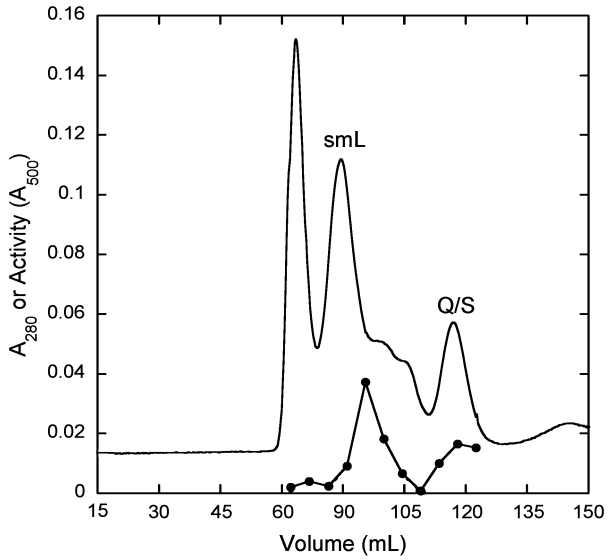

FIGURE 2: Sephacryl S-200 SEC elution chromatogram of the activity-containing fractions from the DEAE column. Activity (●) was measured as A_{500} using the glutamine-dependent Bratton−Marshall assay. Elution of PurS (S), PurQ (Q), and smPurL (smL) are noted.

DTT, pH 7.8) and 1.5 mL of Sigma Protease Inhibitor Cocktail. Cells were then lysed by two passes through a French press at 14 000 psi. Cellular debris was removed by centrifugation at 17 000 rpm for 40 min. Streptomycin sulfate (0.3 volumes, 6% w/v made in S buffer) was then added to the supernatant over 20 min while stirring on ice. The solution was stirred for an additional 20 min and then cleared by centrifugation. DNase I (500 U, Roche) was added to the supernatant, and this solution was allowed to stir at room temperature for 20 min.

The supernatant was next loaded onto a DEAE Sepharose FF (1.5 cm × 25 cm, Sigma) column equilibrated in S buffer. The column was washed with buffer until $A_{280} < 0.1$. A linear gradient (600 × 600 mL) was applied from 25−500 mM NaCl in S buffer. The flow rate was 2 mL/min, and 10 mL fractions were collected. PurS eluted at 50 mM NaCl (Supplemental Figure 1, Supporting Information). Protein from this peak was then concentrated with an Amicon device over a YM-30 membrane (Millipore). The concentrated protein was applied to a Sephacryl S-300 (1.5 cm × 100 cm, Sigma) column equilibrated in S buffer, but the concentration of DTT was lowered to 1 mM. The protein was eluted at a rate of 0.3 mL/min, and 5 mL fractions were collected. PurS eluted as a single peak (Supplemental Figure 2, Supporting Information). The protein was again concentrated with an Amicon device over a YM-30 membrane, followed by a Centriprep YM-30 (Millipore), to 20−40 mg/mL. Glycerol was added to 20% of the final volume, and the protein was rapidly frozen in liquid nitrogen. PurS (13.4 mg/g of cells) was obtained in >95% purity. The purified protein had a mass of 9755 Da by ESI-MS (calculated, 9755 Da). The final protein was quantified using a calculated $\epsilon_{280} = 7680\ M^{-1}\ cm^{-1}$.

Purification of PurQ. pET-PurQ-wt or pET-PurQ-A128T were transformed into BL21(DE3) *E. coli* cells and grown in LB at 30 °C in the presence of 70 μg/mL kanamycin. Cells in 2 L of media were grown in 6 L flasks with shaking at 200 rpm. At an OD_{600} of 0.7−0.9, the cells were induced with 1 mM IPTG and grown for an additional 5 h. The cells were then harvested and frozen in liquid nitrogen.

Both the A128T and wt PurQ proteins were purified using the following procedure based on the purification of *E. coli* HisH (*16*). PurQ activity was monitored at all stages of the purification in the absence of PurS and smPurL using the GDH-coupled glutaminase assay described below.

Cells (13 g) were resuspended in 35 mL of Q buffer (50 mM Tris, 1 mM EDTA, pH 7.4) and then lysed by two passes through a French press at 14 000 psi. Solids were removed by centrifugation at 17 000 rpm for 40 min in a Beckman JA-25.50 rotor.

Streptomycin sulfate (10% w/v in Q buffer) was then added to a final concentration of 1%, and the solution was stirred on ice for an additional 15 min before centrifugation. The supernatant was applied to a DEAE Sepharose FF column (2.5 cm × 10 cm) equilibrated in Q buffer. The column was washed until $A_{280} < 0.1$. A128T PurQ was eluted with a linear gradient (200 × 200 mL) of 0−300 mM KCl in Q buffer. A flow rate of 3 mL/min was employed, and 6 mL fractions were collected. A128T PurQ eluted in the main protein fraction at 100 mM KCl (Supplemental Figure 3, Supporting Information). In contrast, wt-PurQ eluted at 250 mM KCl with a linear gradient (200 × 200 mL) of 0−500 mM KCl in Q buffer (data not shown).

The PurQ fractions were then pooled and diluted 1:1 with 40 mM KP_i, pH 7.0. This solution was applied to a Biogel HTP column (2.5 cm × 5 cm, Bio-Rad) equilibrated in 20 mM KP_i, pH 7.0. The flowthrough and a 40 mL wash were combined and then concentrated with an Amicon device over a YM-30 membrane to 50 mg/mL. This solution (1 mL) was then applied to a Sephacryl S-100 (1.5 cm × 75 cm, Sigma) column equilibrated in 20 mM KP_i, 100 mM KCl, pH 7.0. The column was eluted at 0.2 mL/min, and 5 mL fractions were collected (Supplemental Figure 4, Supporting Information). The protein was then concentrated to 15−30 mg/mL with a Centriprep YM-10 (Millipore). Glycerol was added to a concentration of 20%, and the protein was rapidly frozen

in liquid nitrogen and stored at −80 °C. A typical yield of homogeneous A128T PurQ was 9.1 mg/g of cells. Purification of wt PurQ resulted in a significantly lower yield (1.5 mg/g of cells) of 60% homogeneous PurQ. The purified A128T protein had a mass of 24 816 Da by ESI-MS (calculated, 24 814 Da) and was quantified with a calculated $\epsilon_{280} = 20\,580\ M^{-1}\ cm^{-1}$.

Purification of smPurL. pET-smPurL was transformed into BL21(DE3) *E. coli* cells and grown in LB at 27.5 °C in the presence of 70 μg/mL kanamycin. The cells were typically grown in 2 L volumes with shaking at 200 rpm in a 6 L flask. At OD_{600} of 0.7−0.9, the cells were induced with 1 mM IPTG and grown for an additional 5 h. The cells were then harvested and frozen in liquid nitrogen.

Cells (8 g) were resuspended in 30 mL of SL buffer along with 2 mL of Sigma Protease Inhibitor Cocktail. Cells were then lysed by two passes through a French press at 14 000 psi. Cell debris was removed by centrifugation for 25 min at 17 000 rpm. Streptomycin sulfate (0.2 volumes, 6% w/v in SL buffer) was then added over 15 min while stirring on ice, followed by stirring for an additional 15 min. Solids were removed by centrifugation.

The supernatant was next applied to a DEAE Sepharose FF (2.5 cm × 14 cm, Sigma) column equilibrated in SL buffer. The column was washed until $A_{280} < 0.1$. The protein was eluted with a linear gradient (300 × 300 mL) of 0−500 mM KCl in buffer SL. A flow rate of 4 mL/min was used, and 8 mL fractions were collected. smPurL eluted in the major protein-containing peak at 125 mM KCl (Supplemental Figure 5, Supporting Information). The protein was then concentrated to 20 mL with an Amicon device and a YM30 membrane before dialysis overnight in a 12 kD molecular weight cutoff membrane (Sigma D-0405) against 2 × 500 mL of SL buffer. This protein (diluted to 50 mL) was then applied to a Reactive Red 120 agarose (2.5 cm × 13.5 cm, Sigma) column equilibrated in SL buffer. The column was washed with 2.5 column volumes of buffer at 1 mL/min. smPurL was then eluted by continuing to wash the column with SL buffer at a flow rate of 3 mL/min until $A_{280} < 0.1$. The entire elutate was concentrated with an Amicon device over a YM-30 membrane (Millipore) and a Centriprep YM-50 (Millipore) to a concentration of 20−30 mg/mL. Glycerol was then added to 20%, and the protein was rapidly frozen and stored at −80 °C. A typical yield of smPurL was 4.2 mg/g of cells. The purified protein had a mass of 80 213 Da by ESI-MS, similar to the 80 194 Da mass predicted by removal of the N-terminal methionine revealed by Edman degradation. The purified protein was quantified with a calculated $\epsilon_{280} = 51\,520\ M^{-1}\ cm^{-1}$.

Enzyme Reconstitution. To reconstitute FGAR-AT activity, 2 equiv of PurS, 1 equiv of smPurL, and 1 equiv of PurQ were combined, in that order, in 100 mM Tris, pH 7.5, 5 mM $MgCl_2$ such that the complex concentration was 10−20 μM. The mixture was allowed to equilibrate on ice for 5 min before use and was stable on ice for several hours at these concentrations. Diluted enzyme was prepared from this stock immediately before use.

Enzyme Assays. Enzymatic activity was determined using three different assays: one to monitor FGAM, one for ADP, and one for glutamate. FGAM synthesis was monitored by a coupled assay with his-PurM using the modified Bratton−Marshall assay (*11*). The buffer for the *B. subtilis* enzymes contained the following in a final volume of 400 μL: 50 mM HEPES, pH 7.2, 20 mM $MgCl_2$, 80 mM KCl, 50 mM L-glutamine, 10 mM ATP, 1 mM β-FGAR, and 0.2 U of his-PurM. When the NH_3-dependent activity was determined for smPurL, the glutamine was replaced with 400 mM NH_4Cl. The amount of FGAR was also increased to 2 mM β-FGAR. The reaction was initiated by addition of enzyme and incubated at 37 °C before being quenched by the addition of 100 μL of 1.33 M potassium phosphate/20% trichloroacetic acid (TCA) pH 1.4. The AIR product was then derivatized and quantified as previously described (*17*).

ADP formation was monitored using a coupled assay with PK and LDH. The reaction mixture was identical to that described for the modified Bratton−Marshall assay above except that it contained 0.2 mM NADH, 3 mM PEP, and PK (3.0 U) and LDH (6.75 U) in place of his-PurM. In the NH_3-dependent reactions, the glutamine in the buffer was replaced with 400 mM NH_4Cl. The reaction was initiated with the addition of enzyme and was monitored by ΔA_{340} ($\epsilon = 6200\ M^{-1}\ cm^{-1}$) at 37 °C.

Formation of glutamate was monitored using a continuous glutaminase assay (*18*). The assay buffer was identical to the Bratton−Marshall assay buffer except that 2 mM 3-acetylpyridine adenine dinucleotide (APAD, Sigma) was added to the reaction mixture, and 20 U of GDH was used as the coupling enzyme instead of his-PurM. Since very high glutamine concentrations were used in these assays, the reaction buffer was incubated for 10 min at 37 °C with GDH to oxidize all the contaminating glutamate. The reaction was then initiated with enzyme and incubated at 37 °C. The reaction was monitored by ΔA_{363} ($\epsilon = 9100\ M^{-1}\ cm^{-1}$).

Determination of Kinetic Parameters. The k_{cat} and K_m values were generally determined by varying the concentration of the substrate from 0.2 to 10 times the K_m, while using saturating concentrations of the other substrates. Kinetic parameters were obtained by fitting initial velocity data to eq 3 using nonlinear regression analysis with KaleidaGraph (Synergy) computer software.

$$v = V_{max}[S]/(K_m + [S]) \quad (3)$$

In cases where substrate inhibition was observed, data were fit to eq 4.

$$v = \frac{V_{max}[S]}{\left(K_m + [S] + \frac{[S]^2}{K_i}\right)} \quad (4)$$

Parameters for PurQ were determined using the glutaminase assay in the absence of PurS, smPurL, FGAR, and ATP. The K_m value for glutamine was determined by varying its concentration from 0 to 50 mM.

The kinetic parameters for the NH_3-dependent reaction of smPurL were determined using either the modified Bratton−Marshall assay (NH_3, FGAR) or the PK/LDH coupled assay. The $K_{m,app}$ value for β-FGAR was obtained by varying its concentration from 0 to 8 mM in the presence of 400 mM NH_4Cl and 10 mM ATP. The $K_{m,app}$ for NH_3 was obtained by varying the concentration of NH_4Cl from 0 to 700 mM with 2 mM β-FGAR and 10 mM ATP. Up to 1 U of his-PurM was added to this reaction to offset the effects of NH_4Cl on his-PurM activity. The concentration of NH_3 was

determined using the Henderson−Hasselbalch equation. The $K_{m,app}$ value for ATP was obtained by varying its concentration from 0 to 2 mM using 2 mM β-FGAR and 400 mM NH_4Cl.

Kinetic parameters for the PurS/smPurL/PurQ complex were determined using either the modified Bratton−Marshall assay or the glutaminase assay. All specific activity and kinetic parameter measurements were made at enzyme concentrations of 0.2−0.4 μM using the A128T PurQ mutant. The K_m value for β-FGAR was obtained by varying its concentration from 0 to 8 mM using 10 mM ATP and 25 mM glutamine. The $K_{m,app}$ value for ATP was determined by varying its concentration from 0 to 3.25 mM in the presence of 1 mM β-FGAR and 25 mM glutamine. The $K_{m,app}$ for glutamine was determined by varying its concentration from 0 to 24 mM in the presence of 1 mM β-FGAR and 10 mM ATP.

Metal Ion Dependence. Metal ion dependence (Mg^{2+} and K^+) was measured by using the glutaminase assay since both the his-PurM and PK coupling enzymes are dependent on these ions. The glutaminase buffer consisted of 100 mM Tris, pH 7.2, 2 mM APAD, 10 mM ATP, 1 mM β-FGAR, 25 mM L-glutamine, and 20 U of GDH in a volume of 300 μL. In experiments to examine magnesium dependence, KCl was 80 mM, and the enzyme reconstitution was carried out in Tris buffer without magnesium. The concentration of $MgCl_2$ was varied from 0 to 40 mM. In experiments to test potassium dependence, $MgCl_2$ was at 20 mM, and the concentration of KCl was varied from 0 to 80 mM.

Titrations to Examine the Stoichiometry of the FGAR-AT. Titrations of the FGAR-AT proteins with one another were monitored using the modified Bratton−Marshall assay and could only be successfully performed at enzyme concentrations above 0.1 μM, which required 1 U of his-PurM as a coupling agent.

A. Titrations with PurQ. smPurL (1 nmol) was reconstituted with PurS (2 nmol) and PurQ (0.2−4 nmol) in 100 μL of 50 mM HEPES, pH 7.2, 20 mM $MgCl_2$, 80 mM KCl, 10 mM ATP, and 25 mM L-glutamine. This mixture was allowed to incubate on ice for 5 min. The enzyme was then diluted 50-fold into the Bratton−Marshall assay buffer at 37 °C to initiate the reaction.

B. Titrations with PurS. smPurL (1 nmol) was reconstituted with PurS (0.25−4 nmol) and PurQ (1 nmol) in 100 μL of 50 mM HEPES, pH 7.2, 20 mM $MgCl_2$, 80 mM KCl, 10 mM ATP, and 25 mM L-glutamine. The incubation and enzymatic reaction were then carried out as described with the titration of PurQ.

pH Rate Profile. The pH rate profile was determined with the Goods series of buffers using the modified Bratton−Marshall assay. The buffers used were MES (pH 5.5−6.25), MOPS (pH 6.5−7.0), HEPES (pH 7.25−8.0), TAPS (pH 8.5), and CHES (pH 9.0−9.5). A typical assay in 400 μL contained 100 mM buffer, 1 mM β-FGAR, 10 mM ATP, and 50 mM L-glutamine. The enzyme concentration for these reactions was 0.2 μM. In determining the pH rate profile for the NH_3-dependent reaction, we used 2 mM β-FGAR, 10 mM ATP, and 400 mM NH_4Cl. The amount of PurM used in the assays varied between 0.2 and 2 U to ensure full coupling of the reaction at all pH values.

Product Stoichiometry of FGAR-AT. Product stoichiometry of the FGAR-AT reaction was determined by measuring endpoint concentrations of ADP, glutamate, and FGAM. Enzymes were reconstituted as described above. The enzyme mixture was then diluted 1:40 into 400 μL of 50 mM HEPES, pH 7.2, 20 mM $MgCl_2$, 80 mM KCl, 25 mM L-glutamine, 2 mM β-FGAR, 1.5 mM ATP, and 2.5 U/mL his-PurM at 37 °C. The reaction was allowed to proceed for several minutes before quenching by immersion in boiling water for 2 min. Precipitated protein was removed by centrifugation. Six time points were taken for the stoichiometry determination, and a control reaction containing no FGAR-AT was performed at each time point. The final stoichiometry was determined by averaging the stoichiometries obtained at each time point. In addition, these methods were used to determine the stoichiometry of both the *E. coli* and *S. typhimurium* lgPurLs.

FGAM formation was determined by using the modified Bratton−Marshall assay described earlier to calculate the amount of AIR present in the sample (50 μL).

ADP formation was determined using the PK/LDH assay. The quenched reaction or control (60 μL) was added to 610 μL of 50 mM HEPES, pH 7.2, 20 mM $MgCl_2$, 80 mM KCl, 3 mM PEP, 0.2 mM NADH, 3.0 U PK, and 6.75 U LDH, and the ΔA_{340} was measured. The amount of ADP produced by the FGAR-AT was determined by subtracting the control followed by division by 2 to account for ATP consumed by his-PurM.

Glutmate was measured using two methods with GDH. In the first method, 100 μL of the quenched reaction or control was added to 610 μL of 50 mM HEPES, pH 7.2, 20 mM $MgCl_2$, 80 mM KCl, 2 mM APAD, and 20 U GDH. The reaction was incubated for 30 min at 37 °C and the ΔA_{363}(experimental − control) was measured. In the second method, known concentrations of glutamate were included in the control reactions to generate a standard curve using the method of Lund (*19*).

DON Inactivation of PurQ. A typical reaction (150 μL) contained 20 μM PurQ, 20 μM smPurL, 40 μM PurS, 0.45 mM FGAR, 0.5 mM ATP, 10 mM 6-diazo-5-oxo-L-norleucine (DON), 50 mM KP_i, pH 7.25, 75 mM NaCl, and 5 mM $MgCl_2$ at 25 °C. Inactivation of PurQ alone was carried out in the absence of the other proteins, FGAR, and ATP. The inactivation was monitored as a function of time by removal of 2 μL aliquots, which were diluted into 400 μL of the modified Bratton−Marshall assay buffer. With inactivation of PurQ alone, the assay buffer contained PurS and smPurL as well. The DON-inactivated FGAR-AT mixture was used directly in subsequent SEC experiments without the removal of unreacted DON or substrates.

Analytical SEC to Look for Complex Formation. Analytical SEC was performed at 4 °C using a BioCAD Sprint perfusion chromatography system (Applied Biosystems) or at 25 °C using a Rainin HPLC with an analytical Bio-Silect SEC250 column (300 mm × 7.8 mm, Bio-Rad). The column was equilibrated and eluted in filtered and degassed SEC buffer (50 mM KP_i, 75 mM NaCl, pH 7.25). Protein was applied to the column using a 100-μL injection loop and eluted with a flow rate of 1 mL/min. Bio-Rad gel filtration standards (a mixture of thyroglobulin (670 kD), gamma globulin (158 kD), ovalbumin (44 kD), myoglobin (17 kD), and vitamin B_{12} (1.4 kD)) were injected prior to each set of experiments. Typically, 0.6 mg of protein in 125 μL of buffer was injected. All solutions were filtered with CENTREX spin filters (Schleicher & Schuell). Experiments were also performed

using SEC buffer containing 25 mM L-glutamine and 5 mM $MgCl_2$, 5 mM $MgCl_2$ and 0.5 mM ATP, 5 mM $MgCl_2$, 0.5 mM ADP, and 25 mM L-glutamine, and 5 mM $MgCl_2$, 0.5 mM ATP, and 0.5 mM β-FGAR. In addition, experiments were performed using enzyme that either had been allowed to synthesize FGAM for 5 min at 37 °C before application to the column or had been preincubated with a combination of 0.5 mM ADP, 5 mM $MgCl_2$, and L-glutamine. Approximate values for molecular weight were determined using the gel filtration standards and by linear-regression analysis using the KaleidaGraph software. Activities of proteins eluting from the analytical SEC column were determined using the modified Bratton−Marshall assay to monitor glutamine-dependent FGAM formation. Peak volumes were determined by integration.

SEC to Determine Apparent Molecular Weights. SEC was performed using HiPrep 26/60 Sephacryl S-200 HR (for PurS and PurQ) and S-300 HR (for smPurL and the FGAR-AT complex) columns (Amersham Biosciences) coupled to a BioLogic LP system (Bio-Rad). The columns were equilibrated in either SEC buffer or SEC buffer with 0.1 mM ADP, 5 mM $MgCl_2$, and 25 mM L-glutamine. Samples (500 μL) were loaded at 100 μM each protein alone or 100 μM 2PurS/1smPurL/1PurQ complex and eluted with a flow rate of 0.5 mL/min. Elution was monitored by A_{280}, and elution of the FGAR-AT complex was monitored with the glutamine-dependent Bratton−Marshall assay with fractions collected every 3 mL. Bio-Rad gel filtration standards and his-PurM (a 76 kDa dimer) were used as elution standards, and a standard curve was generated as described above. Standard deviations of observed elution times were calculated from multiple injections of the standards.

RESULTS

Genetic and biochemical studies using crude extracts of *B. subtilis* deletion strains suggested that PurS, smPurL, and PurQ were all required for FGAM synthesis (*7*). Based upon these results, we decided to biochemically characterize these proteins in vitro. Two approaches were taken to obtain active protein: the first examined coexpression methods and the second involved expression of the individual proteins and reconstitution of the complex. The success of each approach was based upon observation of glutamine-dependent FGAM production (Scheme 1) using the modified Bratton−Marshall assay.

Cloning, Coexpression, and Copurification of the FGAR-AT Complex. A variety of different strategies were pursued for coexpression. The A128T PurQ and smPurL were cloned into pACYC-DUET-1, yielding pDUET-LQ. When this construct was transformed into BL21(DE3) *E. coli*, expression of PurQ was ∼20% of soluble protein, while that of smPurL was <1% of soluble protein (data not shown). pDUET-LQ was then cotransformed with pET-PurS. The expression level of PurS was high; however, no expression of PurQ or smPurL was observed (data not shown). Next, pDUET-LQ, pET-PurS, and pET-smPurL were all cotransformed, into BL21(DE3) *E. coli*. Under these conditions, PurS, PurQ, and smPurL were all expressed as soluble proteins (Figure 3). No smPurL or PurQ were detected in the insoluble protein fraction. The crude cell lysate produced FGAM at 0.4 U/mg (Table 1). Given that ∼20% of the total

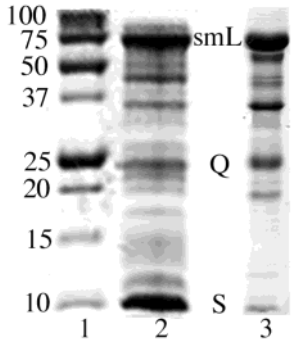

FIGURE 3: SDS−PAGE (15%) of the coexpressed FGAR-AT: lane 1, molecular weight markers; lane 2, soluble crude cell lysate; lane 3, the activity-containing fraction from the DEAE column.

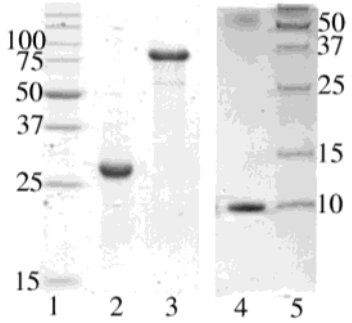

FIGURE 4: SDS−PAGE (12%, lanes 1−3) and tricine (16.5%, lanes 4 and 5) gels of the purified FGAR-AT components: lanes 1 and 5, molecular weight markers; lane 2, PurQ-A128T; lane 3, smPurL; lane 4, PurS. Two micrograms of each protein was loaded.

protein is associated with the FGAR-AT (estimated from SDS−PAGE, Figure 3), activity for the pure protein was estimated at 2−3 U/mg.

Purification of the FGAR-AT complex was attempted using DEAE Sepharose anion-exchange chromatography. During chromatography, the three proteins separated (Figure 1) based on SDS−PAGE analysis. One peak of FGAR-AT activity was observed using the Bratton−Marshall assay. The specific activity of this complex (Figure 3, lane 3) had fallen to 0.27 U/mg due to dissociation of the complex during chromatography (Table 1). The fractions containing activity were pooled and applied to a Sephacryl S-200 SEC column. During elution, smPurL completely separated from PurS and PurQ, which comigrated under these conditions (Figure 2). In addition, only very low levels of activity were recovered (0.013 U/mg, Table 1). Thus, the proteins of the FGAR-AT are weakly associated. These results indicate that any study of the subunit stoichiometry, assembly, and kinetic parameters of the FGAR-AT complex must be carried out by reconstituting the separately purified enzymes or by identification of other components that allow for copurification of the intact complex.

Cloning, Expression, and Purification of the Individual FGAR-AT Components: PurS. The *purS* gene was cloned from *B. subtilis* genomic DNA and ligated into pET-11a. The protein was over-produced in *E. coli* and was purified to homogeneity (Figure 4, lane 4) by DEAE anion-exchange chromatography followed by size exclusion chromatography (SEC) (Supplemental Figures 1 and 2, Supporting Information). Typical yields were ∼13 mg/g of cells. The molecular weight of the protein was confirmed by ESI-MS.

Table 2: Purification of A128T-PurQ

step	protein (mg)	total units (U)	SA (U/mg)	% yield
cell lysate[a]	1159	3.93	0.003	100
streptomycin	1214	1.52	0.001	39
DEAE Sepharose	303	2.14	0.007	54
HTP Biogel	204	3.39	0.02	86
Sephacryl S-100	118	0.590	0.005	15

[a] From 13 g of cells.

Table 3: Purification of smPurL

step	protein (mg)	total units (U)	SA (U/mg)	% yield
cell lysate[a]	800	6.07	0.008	100
streptomycin	778	4.25	0.006	70
DEAE Sepharose	236	5.43	0.02	89
Reactive Red 120 agarose	34	1.11	0.03	18

[a] From 8 g of cells.

Cloning, Expression, and Purification of the Individual FGAR-AT Components: PurQ. The *purQ* gene was also cloned from *B. subtilis* genomic DNA and placed into pSTBLUE-1. The gene was then subcloned into pET-24a for protein expression. *E. coli* containing this plasmid were grown at 30 °C to obtain soluble protein. PurQ was purified on a DEAE Sepharose anion-exchange column (Supplemental Figure 3, Supporting Information). The fractions eluting at 100 mM KCl were pooled, diluted with phosphate buffer, and loaded onto a Biogel HTP column. The flow-through of the column contained PurQ. The eluate was concentrated and loaded onto a SEC column. The resulting PurQ was homogeneous by SDS−PAGE (Figure 4, lane 2) with typical recoveries of 9 mg/g of cells. The activity of PurQ was monitored using the continuous glutaminase assay (Table 2). The variability in total activity is due to removal of an endogenous glutaminase activity from *E. coli* during the purification (Supplemental Figure 4, Supporting Information). The molecular weight of PurQ determined by ESI-MS was 24 816 Da (calculated 24 784), suggesting that the clone contained a mutation.

After purification, the gene was sequenced, which revealed an A128T mutation consistent with the ESI-MS data. This residue is not conserved among PurQ enzymes. To establish the actual identity of this residue, *purQ* was recloned from genomic DNA in five separate reactions using the high fidelity KOD HiFi DNA polymerase. Sequencing of all of the PCR products revealed an alanine at position 128. The wt-gene was also placed into pET-24a. The purification of the wt PurQ protein was carried out as described for the A128T mutant. However, the protein behaved differently from the mutant on DEAE Sepharose, eluting at 250 mM KCl. The purity of wt PurQ (60% homogeneous by SDS−PAGE, data not shown) and recovery were both low. A variety of additional chromatographic methods were examined in an effort to obtain homogeneous protein, all without success. The specific activity of the purified wt-PurQ using the glutaminase assay was 20 nmol min^{-1} mg^{-1}, higher than that of the mutant (5 nmol min^{-1} mg^{-1}). However, the specific activity of the wt-PurQ in the FGAM synthesis assay described later was 10-fold lower (0.12 U/mg vs 1.2 U/mg) than the mutant PurQ. It is possible that the high glutaminase activity of the wt-PurQ could be due to an endogenous *E. coli* glutaminase, as was seen in the SEC purification of the A128T mutant. In the reconstitution experiments described subsequently, the A128T PurQ has been employed.

Cloning, Expression, and Purification of the Individual FGAR-AT Components: smPurL. The *purL* gene was amplified by PCR from the pDE51 sequencing vector and then ligated into pET-24a (*6*). Sequencing of the cloned gene revealed a L513F mutation, which resulted from a single nucleotide mutation (CTC to TTC) in the codon. In contrast with the observations with the *purQ* gene, a similar set of experiments revealed that the wt smPurL contains a phenylalanine at position 513, not a leucine as previously reported (*6*). All work has thus been carried out with smPurL containing F513.

In contrast to the coexpression experiments described above, expression of smPurL alone resulted in aggregation and inclusion bodies. To maximize expression of soluble PurL, *E. coli* containing the *purL* expression plasmid were grown at 27.5 °C. The enzyme was purified using DEAE Sepharose anion-exchange chromatography (Supplementary Figure 5, Supporting Information) followed by chromatography on Reactive Red 120 agarose. The red agarose column removed inactive aggregates of smPurL that eluted in the flowthrough of the column. These aggregates, unable to reequilibrate with active smPurL, accounted for 40% of the soluble smPurL. The active smPurL also flowed through the dye affinity column, but only after the elution of the aggregate. A small amount of smPurL remained bound to the column and eluted at 250 mM NaCl. While recoveries from this column were low (18% of units, Table 3), recovery was sacrificed for purity to enhance crystallographic efforts. The smPurL was typically recovered at 4 mg/g of cells and judged to be 90% homogeneous based on SDS−PAGE (Figure 4, lane 3). N-terminal protein sequencing of smPurL indicated loss of methionine, consistent with the ESI-MS molecular weight. Activity of smPurL (33 nmol min^{-1} mg^{-1}) was monitored using the Bratton−Marshall assay with NH_4Cl as the ammonia source. Under these conditions, PurS and PurQ were not needed for FGAM synthesis.

Reconstitution of Enzymatic Activity. Based on the stability and solubility problems encountered with both PurQ and smPurL, it is perhaps not surprising that reconstitution of FGAR-AT proved to be challenging. Attention to the concentration and ratios of the proteins in the reconstitution mixture, as well as the order of addition of the proteins, was essential. Reconstitutions were carried out on ice to avoid aggregation of both PurQ and smPurL that was observed at higher temperatures (≥25 °C). The concentration of enzymes in the assay mixture was also critical in assessing the success of the reconstitution.

Determination of Subunit Stoichiometry. Initial efforts focused on determination of the stoichiometry of PurS, smPurL, and PurQ required to achieve maximal FGAR-AT activity. After extensive experimentation, successful titrations were shown to require premixing of all three component proteins at ∼10 μM at 4 °C in the presence of glutamine and 10 mM MgATP. It was later determined that the ADP necessary for reconstitution of activity (see below) could be completely supplied by ADP contamination present in the 10 mM ATP (unpublished results). This mixture was then diluted 100-fold into the assay buffer at 37 °C and monitored

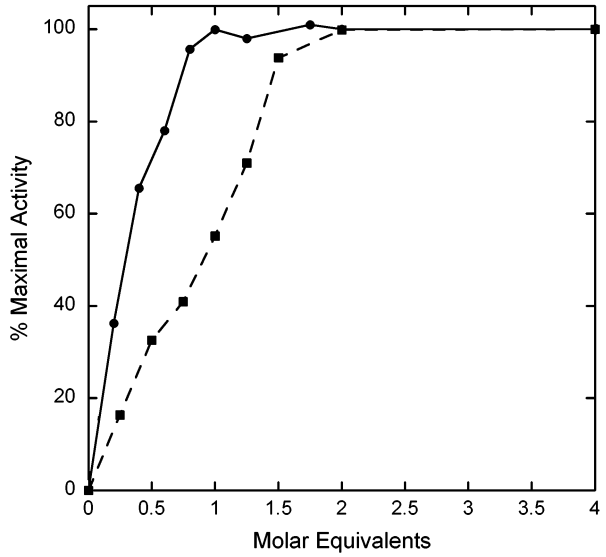

FIGURE 5: Determination of the ratio of PurS/smPurL/PurQ required for maximal activity: (●) 2PurS/1smPurL (10 μM) and variable amounts of PurQ (0−40 μM) were preincubated at 4 °C for 5 min, and the reaction mixture was then diluted 100-fold and assayed for FGAM production; (■) 1 PurQ/1 smPurL (10 μM) and variable amounts of PurS (0−40 μM) were preincubated at 4 °C for 5 min, and the reaction mixture was then diluted 100-fold and assayed for FGAM production.

Table 4: Selected Kinetic Parameters of FGAR-AT Enzymes

property	smPurL[a]	PurQ	FGAR-AT complex[a]	*E. coli*[b]	chicken liver[c]
K_m FGAR	2.5 mM		507 μM	30 μM	100 μM
K_m ATP	398 μM		181 μM	51 μM	1.5 mM
K_m Gln		2.5 mM	1.3 mM	64 μM	40 μM
K_m NH_3	∼3.5 mM			1 M	10 mM
magnesium[d]			20 mM	20 mM	20 mM
potassium[d]			20 mM	10 mM	60 mM
k_{cat} FGAM synthesis (s^{-1})[e]	0.044		2.49	5.00	0.47
k_{cat} glutaminase (s^{-1})[f]		0.002	0.066	0.001	0.002

[a] For smPurL and the FGAR-AT complex, these values are $K_{m,app}$ due to substrate inhibition. [b] Values from ref *11*. [c] Values from refs *21* and *23*. [d] Defined as the concentration of Mg^{2+} or K^+ required for maximal activity. [e] Measured by the rate of FGAM synthesis using either NH_3 or glutamine as the nitrogen source. [f] Measured by the rate of glutamine hydrolysis using the continuous glutaminase assay in the absence of FGAM synthesis. For the FGAR-AT complex, this was measured in the presence of FGAR but not ATP.

for FGAM production. The results of a typical titration of PurQ with PurS and smPurL (2:1) are shown in Figure 5 (●). The titration reveals that maximal activity is achieved at a ratio of PurQ to smPurL of 1:1. PurS was titrated with PurQ and smPurL (1:1) using a similar procedure. Under these conditions, 2 equiv of PurS are needed for maximal activity (Figure 5, ■). These results suggest the stoichiometry of PurS/smPurL/PurQ is 2:1:1.

Steady-State Kinetics. As noted in the Introduction, FGAM synthesis can be divided into two half-reactions (eqs 1 and 2): the hydrolysis of glutamine to glutamate and NH_3 and ATP-dependent amidine formation. Kinetic characterizations of the individual components (PurQ and smPurL), as well as the complex (PurS, smPurL, and PurQ), have been investigated. The results are summarized in Table 4 and are shown in comparison to previously studied lgPurLs.

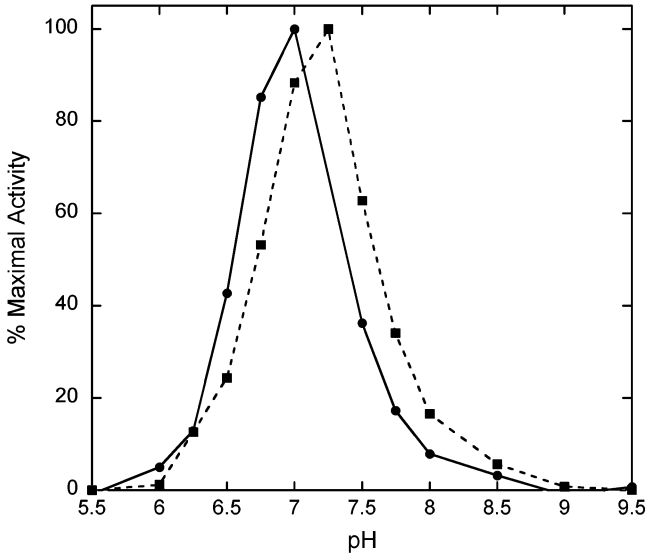

FIGURE 6: pH dependence of the FGAR-AT reaction using either glutamine (●) or NH_3 (■) as the nitrogen source.

Glutaminase Activity of PurQ. PurQ is a member of the triad class of glutaminases that includes PabA (the glutaminase of the PabA/PabB aminodeoxychorismate synthase), HisH (the glutaminase of the HisH/HisF imidazole glycerol phosphate synthase), and the lgPurLs (*11*, *16*, *18*, *20*). In all cases, these enzymes possess very low (or in some cases undetectable) glutaminase activity in the absence of the amidotransferase, other substrates, or both. The kinetic parameters of the A128T-PurQ are summarized in Table 4. As in the case of PabA and the chicken liver lgPurL, a lag phase was present in the kinetics prior to the reduction of APAD (*18*, *21*). The activity of PurQ alone (0.002 s^{-1}) is 0.08% that in the complex. The presence of smPurL, PurS, and MgATP did not increase the activity. However, incubation with smPurL and PurS (2PurS/1PurQ/1smPurL) and β-FGAR increased the turnover 30-fold (0.066 s^{-1}). No additional increase in glutaminase activity was observed upon addition of the ATP analogue β,γ-methyleneadenosine 5′-triphosphate (AMP-PCP).

Amidotransferase Activity of smPurL. smPurL alone can catalyze formation of FGAM in the presence of NH_4Cl with a turnover number of 0.044 s^{-1}, 1.8% the rate of FGAM synthesis using glutamine. This number is similar to those previously reported for the *E. coli* (2%) and chicken liver lgPurLs (5%) (*11*, *22*).

The steady-state kinetic parameters of smPurL with ammonia have been investigated at pH 7.25 (see pH rate profile, Figure 6) and are shown in Table 4. FGAM formation was measured using the Bratton−Marshall assay, and ADP production was measured using the PK/LDH assay. Substrate inhibition was observed at concentrations of NH_4Cl > 400 mM and β-FGAR > 2 mM. While the inhibition seen with β-FGAR could be fit to eq 4, inhibition kinetics observed with NH_4Cl could not be fit to standard inhibition equations. The K_m's reported in Table 4 are therefore apparent K_m's ($K_{m,app}$). Of particular note is the $K_{m,app}$ for NH_3 of ∼3.5 mM. This value is similar to that reported for the chicken liver lgPurL (10 mM) and contrasts dramatically with that reported for the *E. coli* lgPurL (1 M) (*11*, *22*).

Activity of the FGAR-AT Complex. The three assays described above have been used to measure FGAM, ADP, and glutamate formation by the FGAR-AT complex. These assays were performed using the ratio of 2PurS/1smPurL/1PurQ and at protein concentrations of >0.1 μM. At lower enzyme concentrations, the specific activity of the complex dropped sharply (Supplemental Figure 6, Supporting Information). Similar to observations made in the smPurL assays, β-FGAR exhibited substrate inhibition at >2 mM. Consequently, eq 4 was used to fit the data, giving a K_m of 507 μM. Kinetic analyses to determine $K_{m,app}$'s for glutamine and ATP were carried out at 1 mM β-FGAR (Table 4). The FGAR-AT complex gave a turnover number of 2.5 s^{-1}, which is comparable to that of lgPurLs (Table 4). While the assays to measure FGAM and glutamine formation gave complementary results, the coupled PK/LDH assay monitoring ADP formation was problematic. Long lag phases were observed. Similar assays on the *E. coli* and *S. typhimurium* lgPurLs exhibited no lag phases. The source of the lag phase was determined to be associated with the ATP regenerating system because addition of PK and PEP (or, alternatively, creatine kinase and phosphocreatine) resulted in the observation of lag phases in the glutaminase and Bratton−Marshall assays. These results suggested that a small amount of ADP is required for FGAR-AT complex assembly and turnover. The source of the ADP in our assays appears to be from background ATPase activity of the his-PurM coupling enzyme or from ADP contamination of our ATP stocks (A. Hoskins and J. Stubbe, unpublished results).

Metal Ion Dependence. As with both the *E. coli* and chicken liver lgPurLs, the FGAR-AT reaction for the smPurL was found to be metal ion dependent (*11*, *23*). Magnesium is required for the reaction, while saturating potassium levels stimulated FGAM synthesis 5-fold. The optimal magnesium and potassium concentrations were 20 mM. These values are similar to those previously reported for the lgPurLs (Table 4).

pH Dependence of the FGAR-AT Reaction. During our efforts to examine the NH_3-dependent smPurL activity, the assays were initially carried out at elevated pH ($\geq$8.0). Previous studies of the ammonia dependence of many glutamine-requiring enzymes have shown that elevated pH is essential to increase the concentration of available NH_3 (*11*, *16*). At pH 8.0, however, no activity was detected for smPurL. This prompted our studies of the pH-dependence of the FGAR-AT reaction. As shown in Figure 6, the complex has a sharp pH profile with an optimum of $\sim$7.0. The pH rate profile for the NH_3-dependent reaction is very similar to the glutamine reaction with a shift of the pH optimum to pH $\approx$ 7.25. These results indicate that the pH-dependence of this enzyme resides on smPurL.

Stoichiometry of the Reaction. The complexity associated with optimization of the active FGAR-AT caused us to examine carefully the product stoichiometry of the reaction. It was determined to be 1 FGAM/1.1 $\pm$ 0.2 ADP/1.7 $\pm$ 0.2 glutamate, in contrast to the expected results of 1:1:1. The glutamate was quantitated by two independent methods (Experimental Procedures). As a control for this assay, the ratio of FGAM to glutamate formation was determined for the *E. coli* and *S. typhimurium* lgPurLs. It was found to be 1:(1.5 $\pm$ 0.1) and 1:(1.6 $\pm$ 0.1), respectively. These results contrast with the earlier report of 1 ADP/1 glutamate for the chicken liver lgPurL (*21*, *23*). Our results with three bacterial FGAR-ATs indicate that under our assay conditions glutamine hydrolysis is uncoupled from FGAM production.

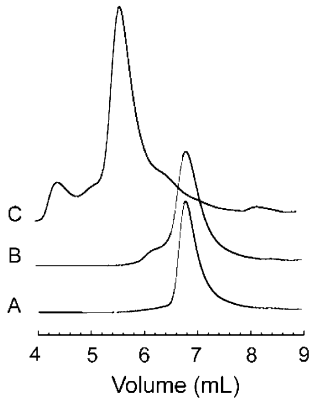

FIGURE 7: Analytical SEC results of the FGAR-AT component proteins injected individually. PurS (A), PurQ (B), and smPurL (C) elute at 6.8, 6.8, and 5.4 mL, respectively. The shoulders on the left-hand side of the PurQ and smPurL peaks represent aggregated protein.

DON Inactivation of PurQ. Support for catalytic coupling of the glutaminase activity to substrate interactions within the smPurL enzyme was sought using the mechanism-based inhibitor 6-diazo-5-oxo-L-norleucine (DON). This compound inactivates many glutaminases by alkylating the cysteine required for covalent catalysis (*20*). PurQ was also inactivated by DON but required the presence of smPurL, PurS, MgATP, and β-FGAR. The half-life for inactivation was <1 s when saturating in all substrates. PurQ mixed with DON alone lost only 70% of its activity after more than 20 h at 25 °C. Therefore, formation of the FGAR-AT complex and binding of MgATP and FGAR accelerates the rate of DON labeling by a factor of 10^4. This rate acceleration is comparable to the 1250-fold increase in glutaminase activity seen upon complex formation and FGAM synthesis (Table 4). This feature is common to all ATs, but it is still not well-understood.

Quaternary Structure of PurS, smPurL, and PurQ Alone and in Complex. Analytical SEC on a Bio-Rad Bio-Silect SEC250 column was used to study the quaternary structure of PurS, PurQ, and smPurL individually and in the FGAR-AT complex. While this column has limited resolution, the small excluded volume was essential for equilibrating the column with substrates (FGAR, glutamine, ATP) to determine whether their presence alters complex formation.

As shown in Figure 7, PurS, PurQ, and smPurL all migrated as discrete species when separately injected. PurS (Figure 7A) and PurQ (Figure 7B) eluted with identical retention volumes of 6.8 mL. smPurL eluted at 5.4 mL (Figure 7C). Thus, complex formation could be monitored by disappearance of the PurS and PurQ peaks and by either an increase in the smPurL peak or the appearance of a new peak in the chromatogram.

In an effort to obtain direct evidence for a FGAR-AT complex, analytical SEC was carried out on PurS, smPurL, and PurQ mixed at different ratios and concentrations in the presence and absence of substrates (ATP, FGAR, glutamine, and Mg^{2+}) and at different temperatures. A typical set of results are shown in Figure 8A. With the proteins alone or in the presence of MgATP, glutamine, or β-FGAR, no

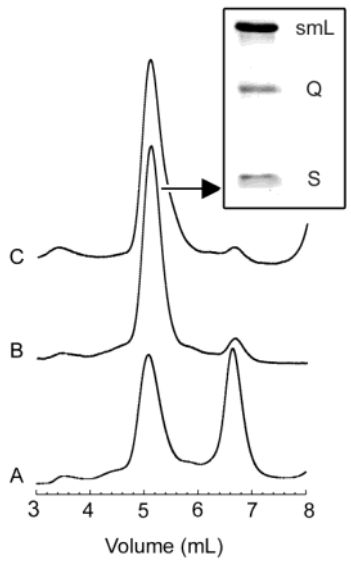

FIGURE 8: SEC evidence for the importance of the small molecules glutamine and ADP in complex formation. In panel A, injection of 2PurS/1smPurL/1PurQ gave complete separation of the components. PurS and PurQ elute at 6.8 mL, while smPurL elutes at 5.2 mL. Inclusion of glutamine, MgATP, MgADP, or β-FGAR gave similar results. In panel B, injection of 2PurS/1smPurL/1PurQ preincubated with glutamine and MgADP and inclusion of glutamine and MgADP in the elution buffer gave complex formation (confirmed by 15% SDS−PAGE, inset). In panel C, injection of 2PurS/1smPurL/1PurQ inactivated with DON and chromatographed with MgADP in the elution buffer also showed complex formation.

evidence of complex formation was seen at either 4 or 25 °C.

Our kinetics studies suggested that MgADP facilitated formation of an active form of the FGAR-AT, an observation further supported by the presence of a tight binding $(Mg^{2+})_3$-ADP in the structure of the lgPurL (*12*). Thus, 2PurS/1smPurL/1PurQ was preincubated with MgADP. Analytical SEC again revealed no complex formation. However, if the complex had been preincubated with MgADP and glutamine and injected onto a column equilibrated with glutamine, a decrease in the PurS/PurQ peak was observed concomitant with an increase in the smPurL peak (Supplemental Figure 7, Supporting Information). The eluted complex had a specific activity of 0.8 U/mg, and the presence of all three proteins was confirmed by SDS−PAGE. Surprisingly, substoichiometric percentages (49%) of PurS and PurQ were present in the complex. Finally, if both the FGAR-AT complex and the column were preincubated with MgADP and glutamine, the FGAR-AT was observed to fully form for the first time (84% of PurS and PurQ complexed) and had a specific activity of 2.1 U/mg (Figure 8B). The requirement for MgADP in the elution buffer suggests that MgADP binding to the FGAR-AT complex possesses a micromolar or greater K_D. These results indicate that complex formation is dependent on the presence of both MgADP and the glutamine substrate.

Previous studies on assembly of channeling complexes in other glutamine-requiring ATs suggested that the presence of a glutamine analogue such as DON facilitated complex formation (*24*). The 2PurS/1smPurL/1PurQ complex was therefore inactivated with DON and examined by analytical SEC in the absence of glutamine. While a complex was seen, it contained only 46% of the included PurS and PurQ (Supplemental Figure 8, Supporting Information). The addition of MgADP to the column elution buffer resulted in 92% of the PurS and PurQ complexed with smPurL (Figure 8C). These results indicate that the DON-inactivated PurQ can also trigger complex formation and suggest that the role of glutamine in complex formation may result from glutamine bound as a thioester. Together this work shows that MgADP and either a covalently or noncovalently bound glutamine are absolutely essential to form the active FGAR-AT complex. A tight, transient complex may form to specifically channel the ammonia released from PurQ. Experiments are currently underway to determine the importance of glutamine-thioester formation to complex formation and FGAM synthesis.

The analytical SEC studies described above allowed us to establish the requirements for PurS/smPurL/PurQ complex formation. However, they failed to give us insight into the apparent MW of the complex due to the limited resolution of the analytical column at high molecular weights. To assess apparent MWs of individual proteins and quaternary structure of the complex, SEC studies were carried out on either S-200 HR (for PurS and PurQ) or S-300 HR (for smPurL and the PurS/smPurL/PurQ complex) columns (Supplemental Figures 9 and 10, Supporting Information). Using S-200 HR, PurS (9.7 kDa) was found to migrate as a 30 kDa species indicating either a trimer or an unusual shape, while PurQ (24.8 kD) was found to migrate as a 23 kDa monomer. smPurL (80 kDa) on S-300 HR migrated in the presence or absence of MgADP in the elution buffer with an apparent MW of 190 kDa indicating that it may be a dimer in solution. The unusual migration properties of smPurL prompted us to examine his-PurM, a dimeric structural homologue of smPurL (38 kDa monomer) (*12*). The his-PurM dimer migrated close to its expected MW of 76 kDa. We also examined the *E. coli* lgPurL (141 kDa) by this method because it would be expected to have a shape similar to the complex, and a MW of 119 kDa was observed (*12*).

The MW of the 2PurS/1smPurL/1PurQ complex was determined with MgADP and glutamine in the elution buffer. While a 2:1:1 and a 4:2:2 complex would be expected to have MWs of 124 and 248 kDa, respectively, the observed MW was 153 kDa. The data in conjunction with the controls (his-PurM, lgPurL) favor a 2:1:1 complex but require the use of additional methods to firmly establish this stoichiometry.

DISCUSSION

Amidotransferases (ATs) are enzymes that catalyze the reaction of ammonia (derived from the amide moiety of glutamine) with a wide range of substrates found in many metabolic pathways to generate an aminated product. Seminal structural experiments on two ATs, phosphoribosyl pyrophosphate AT (PurF, the first step in the purine biosynthetic pathway) and carbamoyl phosphate synthetase (CPS, in the pyrimidine biosynthetic pathway), suggested a general model for all ATs in which the glutaminase activity is located on a domain that is spatially separated from the AT domain (*24*, *25*). The separation between the active sites in the two domains of PurF and CPS is, for example, 20 and 45 Å, respectively (*24*, *25*). The long distance and the biochemical evidence that the "NH_2" moiety of the glutamine amide is

found in the final product requires that ammonia is channeled between these two domains (*26*). The structural composition and the mechanism of formation of the channels within proteins have recently received much attention, but as yet no general principles have emerged (*8*).

The *B. subtilis* FGAR-AT provides an excellent system to study communication between several active sites and ammonia channeling in an AT complex. All ATs contain one of two highly conserved glutaminase domains either fused to the AT domain directly or on a separate polypeptide (*20*). The *B. subtilis* FGAR-AT is unique among all ATs in that the enzyme is composed of three proteins (PurS, PurQ, and smPurL) instead of two. The AT domains themselves, not surprisingly, given the variety of substrates and chemistries, are diverse structurally. Variable affinities between the glutaminase and AT domains of several systems have been reported. In the cases of CPS, TrpEG (anthranilate synthase), and HisHF, the glutaminase domain is tightly bound to the AT, and the subunits remain complexed during purification (*16*, *27*, *28*). In the case of PabAB, the proteins have no detectable affinity at 4 °C by SEC (*18*). However, if PabA and PabB are incubated with glutamine at 37 °C and SEC is performed at 25 °C, complex formation is now observed (*29*). This diversity of domain interactions and the coordination of activities between the domains make the channeling of ammonia even more interesting. This phenomenon dovetails with our laboratory's interest in the importance of channeling of chemically unstable intermediates between successive enzymes in a metabolic pathway, using the purine pathway as a paradigm (*1*).

Efforts to coexpress PurS, PurQ, and smPurL in *E. coli* were successful. However, all efforts to purify an active complex resulted in isolation of only the individual components. Thus, in contrast to HisHF or CPS ATs, the proteins responsible for FGAM production only weakly associate. Interestingly, under the coexpression conditions, the solubility and stability of smPurL were greatly enhanced relative to smPurL expressed alone or in the presence of PurS. These observations suggest that the FGAR-AT components are interacting in the cell.

Our inability to isolate the complex meant that to study the FGAR-AT, the complex had to be reconstituted from its purified components. Expression and purification of PurS were straightforward, while efforts to express and purify PurQ and smPurL were complicated by aggregation. Temperature-dependent studies on PurQ suggested that at 25 °C both wt and A128T mutant PurQ have a tendency to aggregate in an irreversible and rapid fashion. This aggregation may account for our inability to purify wt PurQ. smPurL can also aggregate at 37 °C but on a slower time scale. The propensity of these proteins to aggregate provides an explanation for the difficulties encountered in our efforts to reconstitute the active complex.

We encountered many differences in the purification and enzymatic properties between the A128T and wt-PurQs. The reason for these differences is still unclear. Alanine 128 is a nonconserved amino acid that is located on a solvent-exposed loop in the threading models presented in the accompanying paper (*30*). This loop is not predicted to be involved in either catalysis or complex formation. Thus the effects of the A128T mutation may be indirect and will require more extensive structural characterization of PurQ to be elucidated.

Our reconstitution efforts monitoring glutamine-dependent AT activity allowed us to propose a model in which the active AT contains PurS, smPurL, and PurQ in a ratio of 2:1:1 (Figure 5). Our proposed stoichiometry is supported by the recent structure of the monomeric *S. typhimurium* lgPurL and the structures of the *B. subtilis* and *Methanobacterium thermoautotrophicum* PurSs (*12*, *30*, *31*). In addition, the lgPurL structure contains a tightly bound $(Mg^{2+})_3$-ADP that cannot be removed without protein denaturation (A. Hoskins and J. Stubbe, unpublished results). Thus, our stoichiometry of 1 PurQ/1 smPurL suggests that in the complex there will be only a single glutaminase domain that corresponds to a single active AT site. Our results indicating the necessity of ADP for activity and formation of the FGAR-AT complex suggest that smPurL, like lgPurL, will bind MgADP in a second site.

Interestingly, the *B. subtilis* PurS was observed to be a tetramer in each of the crystal structures presented in the accompanying paper (*30*). These results, in conjuction with our SEC results indicating a 30 kD species, suggested that the active form of PurS may be a tetramer. Extrapolation from the studies of PurS alone suggest that FGAR-AT could exist as a 4PurS/2smPurL/2PurQ complex, which is supported by modeling studies (*30*). To distinguish between a 4:2:2 complex and a 2:1:1 complex also consistent with modeling, SEC was performed. The complex was found to migrate as a 153 kDa species, while 124 and 248 kDa are predicted for the 2:1:1 and 4:2:2 complexes, respectively. While these results support a 2:1:1 complex, a 4:2:2 complex with a nonglobular structure cannot be excluded. Further biophysical experiments are in progress to identify the active form of the *B. subtilis* FGAR-AT.

The stoichiometry of products produced by our reconstitution of the FGAR-AT revealed 1.7 glutamate per ADP and FGAM. This uncoupling propensity is shared by both the *E. coli* and *S. typhimurium* enzymes (this work) but not the chicken liver enzyme (*23*). It is interesting to note that measurements made by Buchanan and co-workers on the chicken liver lgPurL indicated that the glutaminase activity could be drastically uncoupled from ADP formation using several glutamine analogues (*21*). For example, the enzyme hydrolyzed ~5 equiv of γ-glutamylhydroxamate for each ADP consumed at 58% the rate of the normal reaction. Similar observations were found for the hydrazide, methoxyamide, and ester analogues of glutamine, and in all cases, hydrolysis required the presence of both MgATP and FGAR. So despite the 1:1 product stoichiometry observed in the physiological reaction, something unusual is clearly involved with the glutaminase activity of the chicken liver enzyme. The inefficient coupling that we observe in our AT and glutaminase domains differs from expectations based on other ATs and warrants further investigation (*16*, *32*).

An unexpected observation during our studies of the *B. subtilis* FGAR-AT was the striking similarity between this enzyme and the PabAB AT. First, both enzymes exhibit weak affinity between the glutaminase and AT domains at 4 °C, and complex formation is greatly enhanced by the inclusion of glutamine in the column elution buffers (*18*, *29*). Second, just as smPurL requires MgADP for activity, PabB requires a tightly bound tryptophan amino acid (*33*). Third, the structures of lgPurL and PabB indicate that conformational changes are likely to be involved in NH_3 channel formation

Table 5: Comparison of AT Enzyme Amination Rates

enzyme	k_{cat}[a]	ratio Gln/NH_3
PurF + NH_3[b]	139 s^{-1}	
PurF + Gln	80 s^{-1}	0.58
CPS + NH_3[c]	2.9 s^{-1}	
CPS + Gln	3.2 s^{-1}	1.10
HisF + NH_3[d]	8.6 s^{-1}	
HisF + HisH + Gln	9.1 s^{-1}	1.06
PabB + NH_3[e]	2.6 min^{-1}	
PabB + PabA + Gln	42.3 min^{-1}	16.3
E. coli PurL + NH_3[f]	0.08 s^{-1}	
E. coli PurL + Gln	5 s^{-1}	62.5
smPurL + NH_3[g]	0.044 s^{-1}	
FGAR-AT complex + Gln	2.5 s^{-1}	56.82

[a] Defined as the rate of substrate amination using either NH_3 or glutamine as the nitrogen source. [b] From ref *34*. [c] From ref *35*. [d] From ref *16*. [e] From refs *18* and *36*. [f] From ref *11*. [g] This work.

(*12*, *33*). Finally, both enzymes display dramatic drops in k_{cat} when NH_3 is used as a nitrogen source instead of glutamine compared to other ATs (Table 5). Whether these observations reveal general principles underlying transient complex formation in AT enzymes remains to be seen.

The results presented in this paper describe the first biochemical characterization of an FGAR-AT composed of three proteins. The accompanying paper describes the first structural characterization of a lgPurL, a crystallographic hold-out and the protein proposed to be a scaffold for the purine biosynthetic metabolon (*12*). This structure and the structures of several PurSs have lead to a model for the *B. subtilis* FGAR-AT consistent with the biochemistry reported in this paper (*30*). The data together suggest that the FGAR-AT complex and lgPurL enzymes will be structurally very similar. The weak protein interactions observed within the FGAR-AT complex and their ability to change as a function of MgADP and glutamine binding are particularly intriguing. These results clearly demonstrate the role small molecule metabolites can play in altering protein−protein interactions and highlight the importance of studying protein complexes under a variety of physiological conditions. This work provides yet another system in the purine pathway to investigate the importance of channeling of chemically reactive intermediates between transiently interacting proteins.

ACKNOWLEDGMENT

We thank T. Joe Kappock for cloning of the PurQ genes. We thank H. Zalkin for the gift of the pDE51 plasmid. We thank H. Holden for the pET-PurT plasmid.

SUPPORTING INFORMATION AVAILABLE

Details of PurS, PurQ, and smPurL cloning and purification; concentration dependence of the activity of the FGAR-AT; examples of partial complex formation in the presence of MgADP or glutamine; SEC results. This material is available free of charge via the Internet at http://pubs.acs.org.

REFERENCES

1. Kappock, T. J., Ealick, S. E., and Stubbe, J. (2000) Modular evolution of the purine biosynthetic pathway, *Curr. Opin. Chem. Biol. 4*, 567−572.
2. Rudolph, J., and Stubbe, J. (1995) Investigation of the mechanism of phosphoribosylamine transfer from glutamine phosphoribosylpyrophosphate amidotransferase to glycinamide ribonucleotide synthetase, *Biochemistry 34*, 2241−2250.
3. Gooljarsingh, L. T., Ramcharan, J., Gilroy, S., and Benkovic, S. J. (2001) Localization of GAR transformylase in *Escherichia coli* and mammalian cells, *Proc. Natl. Acad. Sci. U.S.A. 98*, 6565−6570.
4. Li, C., Kappock, T. J., Stubbe, J., Weaver, T. M., and Ealick, S. E. (1999) X-ray crystal structure of aminoimidazole ribonucleotide synthetase (PurM), from the *Escherichia coli* purine biosynthetic pathway at 2.5 Å resolution, *Struct. Fold. Des. 7*, 1155−1166.
5. Mueller, E. J., Oh, S., Kavalerchik, E., Kappock, T. J., Meyer, E., Li, C., Ealick, S. E., and Stubbe, J. (1999) Investigation of the ATP binding site of *Escherichia coli* aminoimidazole ribonucleotide synthetase using affinity labeling and site-directed mutagenesis, *Biochemistry 38*, 9831−9839.
6. Ebbole, D. J., and Zalkin, H. (1987) Cloning and characterization of a 12-gene cluster from *Bacillus subtilis* encoding nine enzymes for *de novo* purine nucleotide synthesis, *J. Biol. Chem. 262*, 8274−8287.
7. Saxild, H. H., and Nygaard, P. (2000) The *yexA* gene product is required for phosphoribosylformylglycinamidine synthetase activity in *Bacillus subtilis*, *Microbiology 146* (Part 4), 807−814.
8. Raushel, F. M., Thoden, J. B., and Holden, H. M. (2003) Enzymes with molecular tunnels, *Acc. Chem. Res. 36*, 539−548.
9. Marolewski, A., Smith, J. M., and Benkovic, S. J. (1994) Cloning and characterization of a new purine biosynthetic enzyme: a non-folate glycinamide ribonucleotide transformylase from *E. coli*, *Biochemistry 33*, 2531−2537.
10. Thoden, J. B., Firestine, S. M., Benkovic, S. J., and Holden, H. M. (2002) PurT-encoded glycinamide ribonucleotide transformylase. Accommodation of adenosine nucleotide analogues within the active site, *J. Biol. Chem. 277*, 23898−23908.
11. Schendel, F. J., Mueller, E., Stubbe, J., Shiau, A., and Smith, J. M. (1989) Formylglycinamide ribonucleotide synthetase from *Escherichia coli*: cloning, sequencing, overproduction, isolation, and characterization, *Biochemistry 28*, 2459−2471.
12. Anand, R., Hoskins, A. A., Stubbe, J., and Ealick, S. E. (2004) Domain Organization of *Salmonella typhimurium* Forymylglycinamide Ribonucleotide Amidotransferase Revealed by X-ray Crystallography, *Biochemistry 43*, 10328−10342.
13. Lowry, O. H. R., Nira J., Farr, A. L., and Randall, R. J. (1951) Protein measurement with the Folin phenol reagent, *J. Biol. Chem. 193*, 265−275.
14. Schaegger, H., and Von Jagow, G. (1987) Tricine-sodium dodecyl sulfate-polyacrylamide gel electrophoresis for the separation of proteins in the range from 1 to 100 kDa, *Anal. Biochem. 166*, 368−379.
15. Sambrook, J., Fritsch, E. F., and Maniatis, T. (1989) *Molecular Cloning A Laboratory Manual*, Second Edition, Cold Spring Harbor Laboratory Press, Cold Spring Harbor, NY.
16. Klem, T. J., and Davisson, V. J. (1993) Imidazole glycerol phosphate synthase: the glutamine amidotransferase in histidine biosynthesis, *Biochemistry 32*, 5177−5186.
17. Schendel, F. J., and Stubbe, J. (1986) Substrate specificity of formylglycinamidine synthetase, *Biochemistry 25*, 2256−2264.
18. Roux, B., and Walsh, C. T. (1992) *p*-Aminobenzoate synthesis in *Escherichia coli*: kinetic and mechanistic characterization of the amidotransferase PabA, *Biochemistry 31*, 6904−6910.
19. Lund, P., and Magasanik, B. (1965) *N*-Formimino-L-glutamate Formiminohydrolase of *Aerobacter aerogenes*, *J. Biol. Chem. 240*, 4316−4319.
20. Zalkin, H., and Smith, J. L. (1998) Enzymes utilizing glutamine as an amide donor, *Adv. Enzymol. Relat. Areas Mol. Biol. 72*, 87−144.
21. Li, H. C., and Buchanan, J. M. (1971) Biosynthesis of the purines. XXXIII. Catalytic properties of the glutamine site of formylglycinamide ribonucleotide amidotransferase from chicken liver, *J. Biol. Chem. 246*, 4713−4719.
22. Mizobuchi, K., and Buchanan, J. M. (1968) Biosynthesis of the purines. XXX. Isolation and characterization of formylglycinamide ribonucleotide amidotransferase-glutamyl complex, *J. Biol. Chem. 243*, 4853−4862.
23. Mizobuchi, K., and Buchanan, J. M. (1968) Biosynthesis of the purines. XXIX. Purification and properties of formylglycinamide ribonucleotide amidotransferase from chicken liver, *J. Biol. Chem. 243*, 4842−4852.
24. Krahn, J. M., Kim, J. H., Burns, M. R., Parry, R. J., Zalkin, H., and Smith, J. L. (1997) Coupled formation of an amidotransferase

nterdomain ammonia channel and a phosphoribosyltransferase active site, *Biochemistry 36*, 11061−11068.
25. Thoden, J. B., Holden, H. M., Wesenberg, G., Raushel, F. M., and Rayment, I. (1997) Structure of carbamoyl phosphate synthetase: a journey of 96 Å from substrate to product, *Biochemistry 36*, 6305−6316.
26. Mullins, L. S., and Raushel, F. M. (1999) Channeling of Ammonia through the Intermolecular Tunnel Contained within Carbamoyl Phosphate Synthetase, *J. Am. Chem. Soc. 121*, 3803−3804.
27. Trotta, P. P., Burt, M. E., Haschemeyer, R. H., and Meister, A. (1971) Reversible Dissociation of Carbamyl Phosphate Synthetase into a Regulated Synthesis Subunit and a Subunit Required for Glutamine Utilization, *Proc. Natl. Acad. Sci. U.S.A. 68*, 2599−2603.
28. Zalkin, H., and Hwang, L. H. (1971) Anthranilate Synthetase from *Serratia marcescens*, *J. Biol. Chem. 216*, 6899−6907.
29. Rayl, E. A., Green, J. M., and Nichols, B. P. (1996) *Escherichia coli* aminodeoxychorismate synthase: analysis of *pabB* mutations affecting catalysis and subunit association, *Biochim. Biophys. Acta 1295*, 81−88.
30. Anand, R., Hoskins, A. A., Sintchak, M. D., Bennet, E. M., Stubbe, J., and Ealick, S. E. (2004) A Model for the *Bacillus subtilis* Formylgycinamide Ribonucleotide Amidotransferase Complex, *Biochemistry 43*, 10343−10352.
31. Batra, R., Christendat, D., Edwards, A., Arrowsmith, C., and Tong, L. (2002) Crystal structure of MTH169, a crucial component of phosphoribosylformylglycinamidine synthetase, *Proteins 49*, 285−288.
32. Huang, X., and Raushel, F. M. (2000) Restricted passage of reaction intermediates through the ammonia tunnel of carbamoyl phosphate synthetase, *J. Biol. Chem. 275*, 26233−26240.
33. Parsons, J. F., Jensen, P. Y., Pachikara, A. S., Howard, A. J., Eisenstein, E., and Ladner, J. E. (2002) Structure of *Escherichia coli* Aminodeoxychorismate Synthase: Architectural Conservation and Diversity in Chorismate-Utilizing Enzymes, *Biochemistry 41*, 2198−2208.
34. Chen, S., Burgner, J. W., Krahn, J. M., Smith, J. L., and Zalkin, H. (1999) Tryptophan fluorescence monitors multiple conformational changes required for glutamine phosphoribosylpyrophosphate amidotransferase interdomain signaling and catalysis, *Biochemistry 38*, 11659−11669.
35. Huang, X., and Raushel, F. M. (1999) Deconstruction of the catalytic array within the amidotransferase subunit of carbamoyl phosphate synthetase, *Biochemistry 38*, 15909−15914.
36. Walsh, C. T., Erion, M. D., Walts, A. E., Delany, J. J., 3rd, and Berchtold, G. A. (1987) Chorismate aminations: partial purification of *Escherichia coli* PABA synthase and mechanistic comparison with anthranilate synthase, *Biochemistry 26*, 4734−4745.

BI049127H